Heliyon 8 (2022) e12084

Contents lists available at ScienceDirect

Heliyon

journal homepage: www.cell.com/heliyon

Research article

Characterization of conidial autofluorescence in powdery mildew

Xinze Xu [1], Wenbo Liu [1], Ao Guo, Zekun Shi, Xiaobei Ji, Mengyu Fan, Xiaoli Li, Jinyao Yin, Zhigang Li, Xiao Li, Chunhua Lin, Weiguo Miao [*]

School of Plant Protection/Key Laboratory of Green Prevention and Control of Tropical Plant Diseases and Pests, Ministry of Education, Hainan University, Haikou, 570228, China

ARTICLE INFO

Keywords:
Autofluorescence
Conidia
Powdery mildew
Fluorescence spectrum
Erysiphe quercicola

ABSTRACT

Autofluorescence is produced by endogenous fluorophores, such as NAD(P)H, lipofuscin, melanin, and riboflavin, indicating the accumulation of substances and the state of energy metabolism in organisms. As an obligate parasite, powdery mildew is wildly spread by air and parasitic crops. However, most identification studies have been based on morphology and molecular biology which were far too time- and labor-consuming, thus lacking characteristic, simple, and effective means. Using microscopy under the blue and cyan channels, we elaborated visible conidial autofluorescence in three powdery mildew species, *Erysiphe quercicola*, *E. cichoracearum*, and *Podosphaera hibiscicola*, with a sharp increase during the conidia senescence in *E. quercicola*. Additionally, the main spectral excitation detected by fluorescence spectrometery was 375 nm for these species, with a common emission peak at approximately 458–463 nm, and an additional trend at 487 nm for *P. hibiscicola*. Because NAD(P)H has a similar spectral feature, we further investigated the relation between NAD(P)H and conidial autofluorescence by fluorescence spectra. We observed that the reduced coenzymes prominently contributed to conidial autofluorescence; however, the conidial autofluorescence in *P. hibiscicola* displayed a different trend that may be affected by the oxidized coenzyme –NAD. Finally, the normalized average spectra of these three powdery mildew species and standard samples showed that the spectral trend of each species was similar but that the features in detail were specific and distinct based on principal component analysis. In conclusion, we showed and characterized conidial autofluorescence in three powdery mildew species for the first time. The specific conidial autofluorescence in these species provides a new idea for the development of field spore capture and identification devices for the discrimination of powdery mildew at the species level.

1. Introduction

Autofluorescence is produced by endogenous fluorophores under the appropriate excitation wavelength and can be observed in cell structures and organelles of various organisms [1]. Biomolecules, namely collagen, elastin, keratin, flavins, NAD(P)H, melanin, chlorophyll, lignin, and xanthophyll, can generally be excited individually or in combination. These molecules are also involved in the metabolic state and physiological response. For examples, the NAD(P)H/NAD(P)$^+$ ratio represents energy metabolism and the redox state [2]; FAD indicates the energy metabolism [3]; riboflavin reflects the cofactor component of FAD, FMN, and flavoproteins [4]; lipofuscin is related to peroxidized lipids and protein aggregates associated with oxidative stress [5]; ergosterol is used for measuring fungal biomass [6]; melanin implies virulence and defense against environmental stress [7]; and carotenoids denote anti-oxidative pigments [8]. Unlike exogenous fluorescent additives, endogenous fluorophores have a stable expression and a specific source under certain conditions. Thus, noninvasive monitoring fluorescent molecules can provide insights into making the dynamic processes in organisms visible [9].

Traditional methods of monitoring fungus by staining and morphological observation are labor-intensive and labeled invasive in that they may cause sample poisoning and structure damage. Fluorescent probes and antibodies are used in live cell imaging and biomolecule localization for monitoring gene expression at the spatial and temporal levels [10, 11]. Furthermore, various fluorescence-labeled proteins (e.g. eGFP, mCherry, and YFP) have become critical tools for enabling the localization of protein *in vivo*. However, transferring fluorescence labeled target genes through specific vectors may affect the viability of and be toxic to some organisms. Additionally, the expression of report genes is often

* Corresponding author.
E-mail address: miao@hainanu.edu.cn (W. Miao).
[1] Xinze Xu and Wenbo Liu contributed equally to this work.

https://doi.org/10.1016/j.heliyon.2022.e12084
Received 3 April 2022; Received in revised form 6 August 2022; Accepted 25 November 2022

invisible or unstable [12]. By contrast, autofluorescence originating from endogenous fluorophores in organisms is a natural indicator, and these limited autofluorescent biomolecules have a fixed distribution. For example, combined with label-free fluorescence microscopy and spectrometer, detecting the distribution of intracellular components and monitoring the metabolic status of mycelium were realized in corn pathogenic fungi, arbuscular mycorrhizal fungi, brown-rot fungus, and bacteria [13, 14, 15, 16].

Endogenous fluorescence must be excited under a specific wavelength to achieve the greatest extent of excitement, which makes relevant research targeted and selective. This characteristic autofluorescence method has been applied in the literature. Spore autofluorescence was reported in *Sphagnum* and used to assess the maturity of sedimentary organic matter [17]. Autofluorescence of fungi was also used to assess arbuscular mycorrhizal colonization in mycorrhizal roots [18]. Autofluorescent molecules of pathogens characterized by multiple autofluorescence spectra at the species level were employed as a diagnostic indicator [20]. Autofluorescence in *Diachea leucopodia* was found in the peridium that surrounded the spores and capillitium [19]. Exploratory and applied research has been increasing, such as that on macroscale fluorescence imaging for microorganisms, in identifying porcine cornea infected by bacteria and fungi using autofluorescence [21, 22], and FRET-SLiM and native autofluorescence to study interactions between fluorescent probes and lignin [23]. In our previous study, 57 conidial samples of powdery mildew were collected from Yunnan, Hainan, and Guangdong provinces in China [25]. All the powdery mildew conidia showed an autofluorescence phenomenon.

In this study, we selected three representative powdery mildew species: *Erysiphe quercicola*, *E. cichoracearum* and *Podosphaera hibiscicola*, and two species isolated from rubber trees: *Colletotrichum siamense* and *Lasiodiplodia theobromae* to observe and compare fluorescence intensity. Next, we used the three powdery mildew species to further characterized conidial fluorescence spectra. The conidial autofluorescence intensity produced by *E. quercicola* was found to be closely related to its aging process. Furthermore, our analysis of conidial spectral features indicated that the autofluorescence source was related to NAD(P)H. The conidial autofluorescence features were separated into three clusters by principal component analysis (PCA), suggesting that their spectral difference can be used to differentiate between spores at the species level. Moreover, the distance between the samples in the 2D score plot reflects the contribution degree of NAD(P)/NAD(P)H. Thus, our study characterizes the conidial autofluorescence at the species level, and provides a new method for fungal spore identification.

2. Materials and methods

2.1. Fungal culture and induction of sporulation

In total 57 conidial samples of powdery mildew which infect rubber trees were collected in Hainan, Yunnan, and Guangdong provinces, and most of them displayed autofluorescence in a certain degree. Three species of powdery mildew were selected for further study, namely *Erysiphe quercicola* strain HO-73, *Erysiphe cichoracearum* strain UCSC1, and *Podosphaera hibiscicola* strain HN-01, and inoculated on the leaf surfaces of moderately susceptible rubber tree cultivar Reyan 7-33-97, high-yield agricultural cowpea, and *Arabidopsis pad4* mutant, respectively. A large number of conidia were produced and collected after 14–28 days. *Colletotrichum siamense* strain HN08 and *Lasiodiplodia theobromae* strain HN01 was inoculated on PDA and cultivated at 28 °C and scraped off the hyphae after 3 days to induce sporulation. The collected samples were suspended with sterile water and filtered through Miracloth filter cloth (Merck KgaA, Germany), then centrifuged at 10,000 rpm for 3 min to collect the precipitate. The supernatant was removed, and the precipitate was washed twice with sterile water, then resuspended and diluted to the final concentration of 10^5 CFU/mL.

In order to keep the freshness and natural state of samples, 10 mg solid conidia of each powdery mildew species were collected directly from the leaf surfaces of living plants, and the measurements of fluorescence spectra were performed immediately.

2.2. Autofluorescence intensity measurement

A drop with 10–20 μL suspension on glass slide was used for microscopy observation and photographing. The photos were captured under Red, Green, Blue, and Cyan channels by Olympus BX53 microscope equipped DP80 CCD and U-HGLGPS light source (Olympus Corporation, Japan). Table 1 list the parameters of four channels and photos were taken with an exposure time of 100 ms under each channel. Three biological replicates each consisting of 10 individuals, were used for each species. The fluorescence intensity was calculated by ImageJ (National Institutes of Health, USA), and the gray value was used to represent the intensity. The variable of comparisons was single-factor to ensure the accuracy of the experiments.

2.3. Conidial fluorescence spectra measurement

The fluorescence spectra of solid conidia from powdery mildew were measured by F-7000 Fluorescence Spectrophotometer (HITACHI, Japan) and the samples were held by solid powder clamps (Orient KOJI Ltd, China). The excitation (Em = 455 nm) and emission spectra (Ex = 375 nm) of *E. quercicola*, *E. cichoracearum*, and *P. hibiscicola* conidia were recorded from 300–430 nm and 400–700 nm, respectively, with a spectral resolution of 1 nm, 1200 nm/min scan speed, 10 nm slit, and 400 V PMT. Each sample was measured for five times and the average value was presented. Prepare aqueous solutions of 0.02 M NAD, NADP·Na_2, NADH·Na_2, and NADPH·Na_4 to generate corresponding excitation and emission spectra, respectively, with the same parameters as above.

2.4. Statistical analysis

Statistical analysis was performed with SPSS, and $p < 0.05$ was considered as significant difference between the compared data. Figures were generated with EXCEL (Microsoft, USA), Origin 2021b (education version, OriginLab, Northampton, Massachusetts, USA), and Adobe Photoshop (Adobe, USA). PCA analysis was performed by Principal Component Analysis for Spectroscopy app in Origin Origin 2021b, and spectral data were z-score normalized.

3. Results

3.1. Autofluorescence intensity of phytopathogenic fungal spores

The micrographs of spores from *Erysiphe. quercicola*, *E. cichoracearum*, *Podosphaera. hibiscicola*, *Colletotrichum. siamense*, and *Lasiodiplodia theobromae* under four channels are shown in Figure 1. Although *E. quercicola*, *C. siamense*, and *L. theobromae* are pathogenic fungi of rubber tree leaves and live in the same ecological environment, conidia of *E. quercicola* displayed the strongest autofluorescence, especially under the blue and cyan channels. By contrast, the conidia of *C. siamense* and *L. theobromae* did not show autofluorescence (Figures 1 and 2B). Similar to the autofluorescence of *E. quercicola*, that of *E. cichoracearum*, and *P. hibiscicola* conidia were also observed under the blue and cyan channels, indicating that autofluorescence may be a common phenomenon of powdery mildew (Figures 1 and 2A). Although the morphologies were

Table 1. Fluorescence channel parameters.

Fluorescence channel	Excitation filter/nm	Emission filter/nm	Dichroic filter/nm
Red	530–550	575IF	570
Green	470–495	510–550	505
Blue	360–370	420–460	410
Cyan	400–440	460IF	455

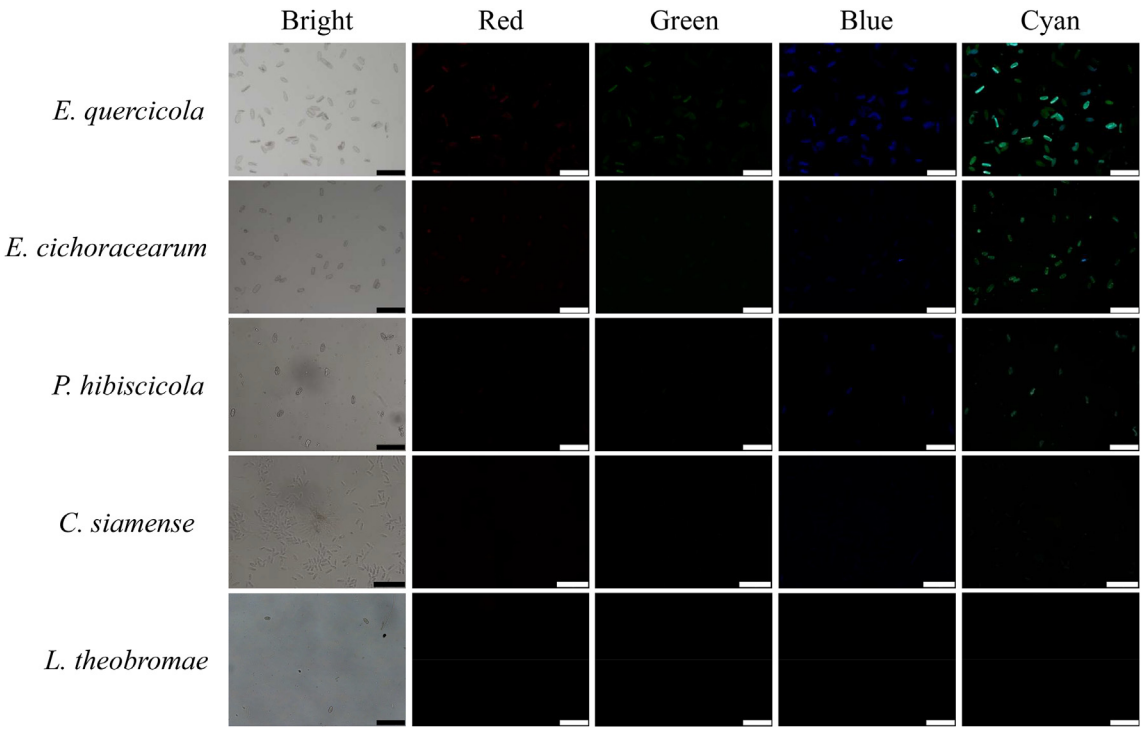

Figure 1. Conidial autofluorescence observation of *E. quercicola*, *E. cichoracearum*, *P. hibiscicola*, *C. siamense*, and *L. theobromae* under the four fluorescence channels. Bar = 100 μm.

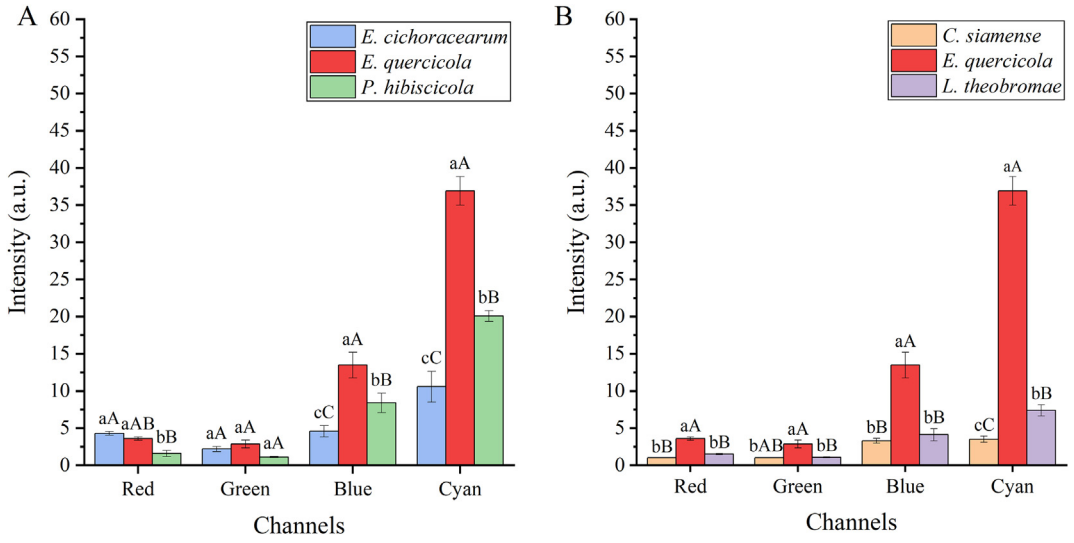

Figure 2. Comparison of the conidial autofluorescence intensity. A. Conidia of *E. quercicola*, *E. cichoracearum* and *P. hibiscicola* at the same culture period. B. Conidia of *C. siamense* and *L. theobromae* at the same culture period. Notes: The weak fluorescence intensity of conidia that cannot be counted under the red and green channels was defined as 1. Different uppercase letters represent $P < 0.01$, different lowercase letters represent $P < 0.05$, and the same letters present there no statistical significance between them.

extremely similar in powdery mildew, *E. quercicola* conidia had an obvious high state ascribable to the substantial accumulation of endogenous fluorophores, and thus could be distinguished from the others.

The morphology of conidia changed with the development stage. Next, we investigated the changes in conidial autofluorescence at different growth stages. The morphology of *E. quercicola* spores changed greatly at the fresh, shrink, and aging stages, and fluorescence intensity changed accordingly (Figure 3A). We observed the aging of conidia and found extremely strong autofluorescence under the cyan channel, that distribution changed from being in the membrane and the cytoplasm to being in the whole spore with the aging of *E. quercicola* conidia, and that autofluorescence also gradually increased under other channels (Figure 3B). To show the trend of autofluorescence, we collected and measured samples at 0, 7, 14, 21, and 28 days after culture. The fluorescence intensity evidently showed an upward trend, indicating that endogenous fluorophores in conidia accumulated or increased during the aging process (Figure 3C).

3.2. Spectral characterization and source exploration of autofluorescence in powdery mildew

To characterize the features of the conidial autofluorescence and explore the sources, we conducted the spectra scan for three species causing powdery mildew. After multiple attempts, the maximum

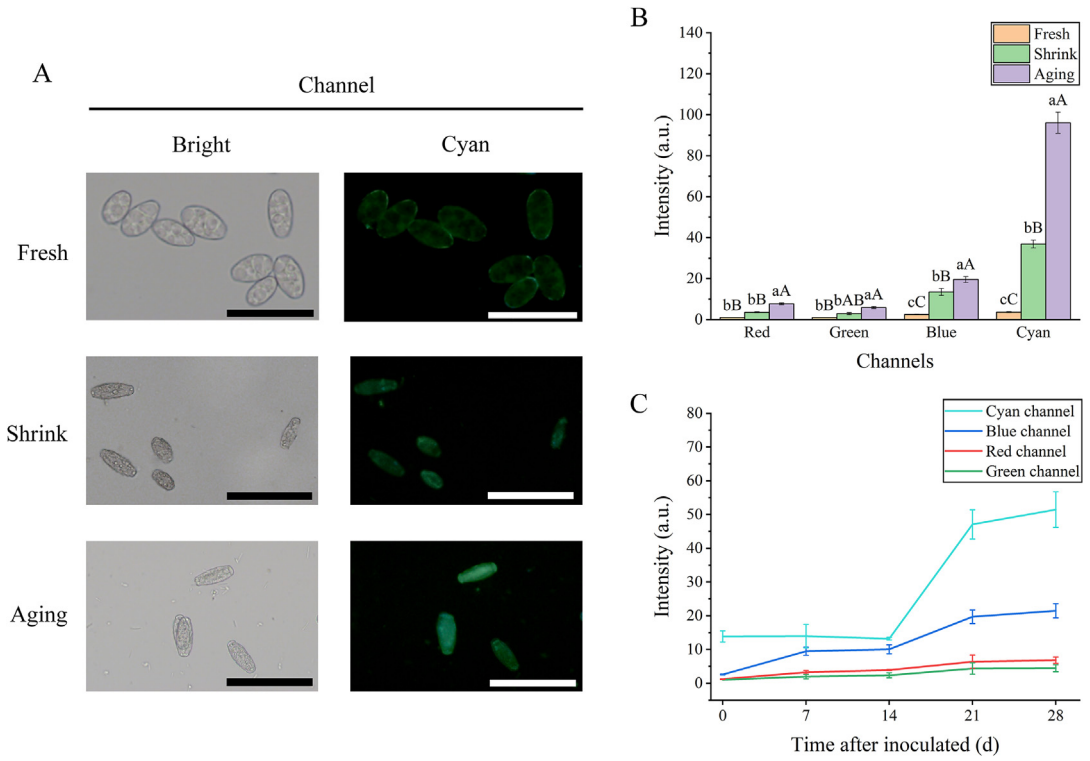

Figure 3. Autofluorescence changes of the *E. quercicola* conidia and intensity statistics. A. Autofluorescence of fresh, shrunk, and aging *E. quercicola* conidia, cyan fluorescence channel as an example. Bar = 50 μm. B. The intensity contrast of the three morphology of *E. quercicola* conidia under the red, green, blue, and cyan fluorescence channels. All comparisons were only performed between different morphology under the same channel. (Different uppercase letters represent $P < 0.01$, different lowercase letters represent $P < 0.05$, and the same letters present there no statistical significance between them). C. Changes of autofluorescence intensity of *E. quercicola* conidia at 0, 7, 14, 21, 28 days.

emission and excitation efficiency for *E. quercicola* were 375 nm and 455 nm, respectively. Consistent with the results of fluorescence intensity in *E. quercicola* conidia, the excitation and emission spectrum of the powdery mildew population presented the strong intensity of the peaks (Figures 4A and 4B). Although the fluorescent spectra of powdery mildew differed fluorescence intensity, we observed a common peak at 460 nm and a broad excitation band in the emission spectra and excitation spectra, respectively (Figures 4A and 4B). Unexpectedly, the emission spectrum of *P. hibiscicola* conidia demonstrated an extra trend, in addition to the intensity difference, as compared with the emission spectra of *E. quercicola* and *E. cichoracearum*.

Additionally, the use of single excitation and emission wavelengths for different samples could affect the maximum intensities they can achieve. To ensure experimental rigor that eliminated the influence of inappropriate wavelengths, we generated the excitation and emission spectrum by using the corresponding maximum emission and excitation wavelength in each species and confirmed our results (Supplement Figure 1A and 1B).

The characteristics of the conidial spectrum of *E. quercicola* were similar to those of NAD(P)H, indicating that NAD(P)H is possible the source of autofluorescence. To verify this hypothesis, we measured the fluorescence spectra of NAD(P) and NAD(P)H materials, including NAD, NADP·Na_2, NADH·Na_2, and NADPH·Na_4 (aqueous solution). A study demonstrated that the difference in UV absorbance between NADH and NAD^+ could be used to evaluate the redox state of mitochondria [26]. However, we found that the difference not only existed in absorption spectra but also in fluorescence emission spectra (Figure 4C). The corresponding maximum excitation wavelengths were selected to generate the emission spectra. NADH·Na_2 and NADPH·Na_4 showed emission peaks at 463 nm and 466 nm, respectively (Figure 4D), with wavelengths and trends of peaks similar to those of conidia in *E. quercicola*. Only the distinctive trend and weak peaks were observed in the emission spectrum with NAD, and NADP had no observable emission peak, indicating that no relationship with the autofluorescence phenomenon was observed. These results suggest that reduced coenzymes probably contributed to conidia autofluorescence in powdery mildew, and NAD may be involved.

Figure 5A showed normalized features of these samples' spectra under 375 nm excitation and further confirmed our hypothesis regarding the source of autofluorescence from spectral peaks position and trends. Used as a dimensionality reduction analysis, PCA clustered together spectra with similar characteristics in the score plot. In this work, we easily discriminated the three powdery mildew species at the species level. As shown in the score plot (Figure 5B), conidial spectra represented by dots of three species were divided into three clusters based on their conidial emission peaks. Moreover, the relative position between the species and standard samples reflected the correlation of the contribution extent to conidial fluorescence. Given the results we have outlined, NADP·Na_2 was not the source and NAD played a role in autofluorescence.

4. Discussion

The autofluorescence phenomenon has been found in various fungi and their spores. Fungal spores are propagules for succession and spread, and the autofluorescence changes in spores are related to their metabolic state during the life process. However, the fluorescence intensity measurement was restricted by many factors. First, the excitation efficiency of mercury lamps differs by band. Second, the fluorescent signal detector has specific sensitivity under certain channels that also interferes with fluorescence intensity and gray values. Third, the selective transmission of the filter on the fluorescence microscope should also be considered. For instance, the channel of cyan and blue are equipped with longwave-pass filters and shortwave-pass filters (Table 1), respectively, thus, conidial autofluorescence has a larger integral area under the cyan channel and provides a stronger fluorescence. However, this explanation

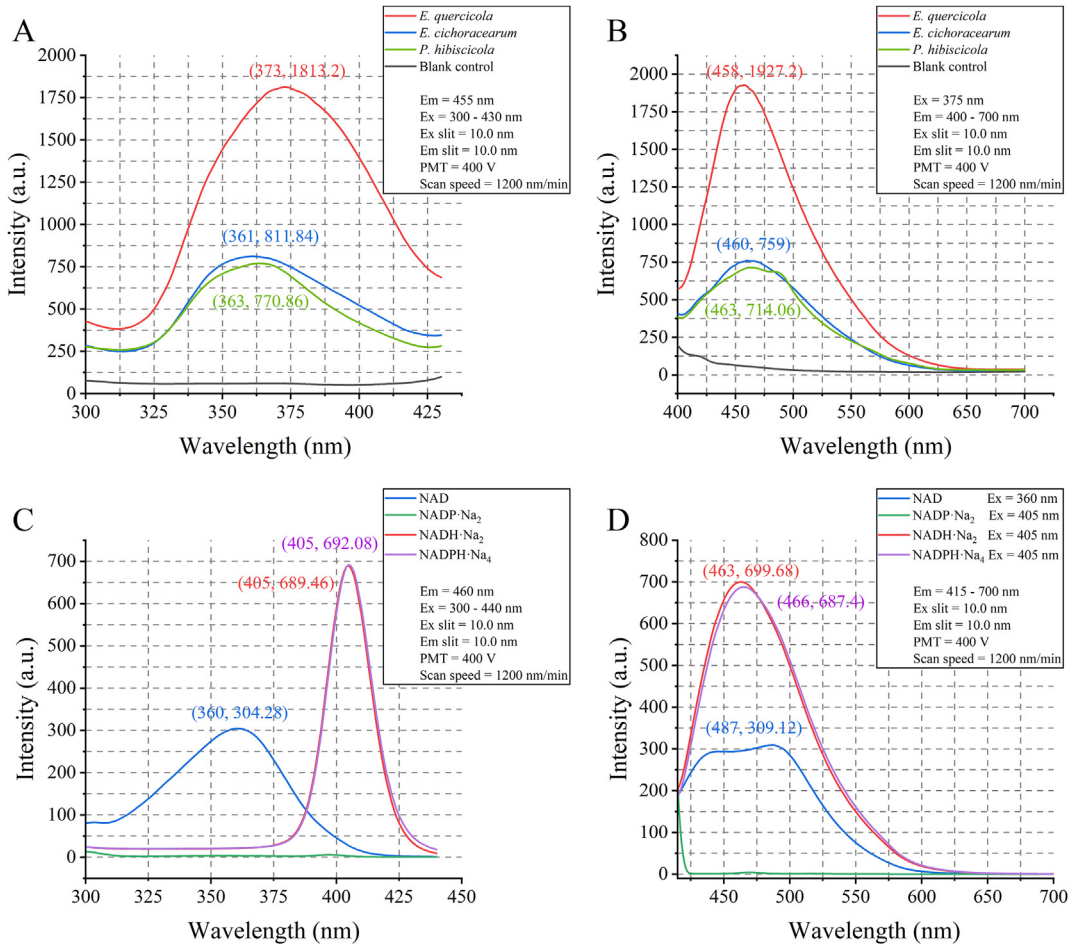

Figure 4. Spectral characterization results (spectral resolution = 1 nm). A. Excitation spectra of *E. quercicola*, *E. cichoracearum*, and *P. hibiscicola* conidia under 455 nm emission wavelength. B. Emission spectra of *E. quercicola*, *E. cichoracearum*, and *P. hibiscicola* conidia under 375 nm excitation wavelength. C. Excitation spectra of NAD, NADP·Na_2, NADH·Na_2, and NADPH·Na_4 under the 460 nm emission wavelength. D. Emission spectra of NAD, NADP·Na_2, NADH·Na_2, and NADPH·Na_4 under their respective maximum excitation wavelengths.

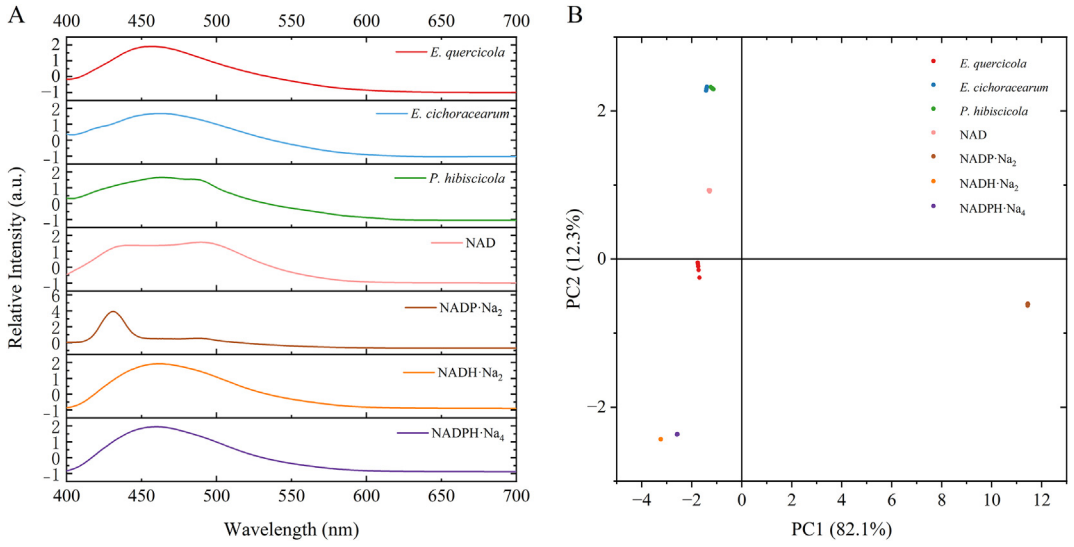

Figure 5. PCA analysis of three powdery mildew species and standard samples. A. The z-score normalized average emission spectra of *E. quercicola*, *E. cichoracearum*, *P. hibiscicola*, NAD, NADP·Na_2, NADH·Na_2, and NADPH·Na_4. B. PCA score plot at the spectral range of 400–700 nm.

cannot demonstrate the conclusion that the blue fluorescence emitted by spores is weaker than that of cyan fluorescence because the blue channel only covers a small range (420–460 nm) emission. Therefore, theoretical conidial autofluorescence under the cyan channel at a 460 nm emission peak corresponds to the color blue actually. To ensure the accuracy of the experiment, we conducted the comparisons under the same fluorescence channel under the same conditions and parameters, and used a single-factor variable.

As an obligate parasitic fungus, powdery mildew has two characteristics that make identifying the pathogenic species difficult: it cannot be cultured in vitro, and it has a crossover of host ranges and similar symptoms in the process of morphological identification. Approximately 10,000 species of plants worldwide can be infected by 650 species of powdery mildew. During the identification and taxonomic research of powdery mildew, researchers have found that one powdery mildew species can infect several hosts, and one host may be infected by various powdery mildew species [24]. The infection of powdery mildew has caused sustained and extensive damage to crops, fruits, and vegetables. Moreover, the conidia of powdery mildew are mainly spread by air currents. Therefore, the identification and detection of powdery mildew spores in the air or on the surface of host plants are essential for controlling powdery mildew infection. Methods used to identify fungi at the species level are mainly based on the host range, polygene tandem phylogenetic tree, and morphology. Traditional morphology methods are combined with, for example, Koch postulates, dyeing, and specific sporulation structure. Although genetic methods based on universal primer ITS1/ITS4 can be identified at the species or genus level within a certain range [27], the contamination during sample collection, the sample volume required, and the time cost must be considered [28].

In this study, we showed that conidial autofluorescence provides a new possibility for rapid identification and development of specific automatic capture and recognition devices. Although *E. quercicola*, *E. cichoracearum*, and *P. hibiscicola* are close interspecies, and their conidia are similar in appearance and size, their conidia do not produce similar autofluorescence. Conidia with mean autofluorescence intensity greater than 5 and 10, represented by grayscale values, could be selected as the positive control, under the blue and cyan channel, representatively. In further trials, the difference between *E. quercicola* and *E. cichoracearum* was only shown in intensity, but *P. hibiscicola* was specific with additional plateaus from 479 to 485 nm, which indicated that the fluorescent sources between them were inconsistent despite causing the same disease. Both the characteristic spectral library and the specific intensity range can be selected as a positive control and have the potential to discriminate at the species level synchronously. Relative to gene sequence analysis and morphology, autofluorescence demonstrated a substantial advantage in time and cost, even without using sample processing in the spectral scan.

For such a specific phenomenon, the standard procedure must be investigated to construct accurate models. The workflow is as follows: observe disease symptoms and determine the host range, identify the genus by the morphological description of structures and spores, and evaluate the maximum probability at the species level by comparing autofluorescence intensities and spectral characteristics. Thus, a wider range of species than has been used in this study should be added, and a database should be built for recording the maximum or minimum intensity of conidial autofluorescence for each of them. In addition, to improve the automation of pathogen monitoring, the automatic identification and analysis system based on the spore capture device using the improved algorithm can diagnose and classify targets. Intelligent spore capture and analysis systems for plant pathogens are usually equipped with bright field imaging. Other solutions, which consider different environmental conditions, could be the combination of existing devices with the fluorescence system. Autofluorescence and spectral characteristics of conidia also provide a new possibility for automatic, accurate, and rapid identification.

Biochemically, the endogenous fluorophores of the fungi are closely related to energy metabolism or pathogenesis and defense mechanisms. Various endogenous fluorophores, including flavins, NAD(P)H, FAD, lipofuscin, ergosterol, carotenoids, and melanin, have been discovered in fungi [29]. NAD(P)H, as a hydrogen and electrons donor, participates in many biochemical cycles such as reductive biosynthesis, and NADH is usually used in the oxidation of the respiratory chain to produce ATP. According to early reports, the emission peak at 460 nm was contributed by NAD(P)H specifically [2, 26, 30, 31, 32]. We found that endogenous fluorophores accumulated during the aging process in *E. quercicola*. The fluorescent spectrum of conidia is also approximately 460 nm and indicates that the source of conidial autofluorescence in *E. quercicola* could be contributed by NAD(P)H. From the aspect of autofluorescence distribution, cytoplasm and mitochondria were considered to be the sites where NAD(P)H exists and cell respiration occurs [26]. However, we found that autofluorescence was distributed in the membrane and cytoplasm at the fresh stage, and changed to evenly distributed inside in senescence owing to shrinkage caused by the loss of vacuoles and moisture. Therefore, we speculate that the autofluorescence source was the single-family rather than comprehensive compounds. NADH and NADPH contribute differently to autofluorescence. In the literature, whether the autofluorescence was from NADH or NADPH was indistinguishable [33]. To further confirm the source of autofluorescence, we characterized the fluorescent spectra of two oxidized coenzymes, NAD and NADP·Na_2, and two reduced coenzymes, NADH·Na_2 and NADPH·Na_4. The excitation spectra of NADH·Na_2 and NADPH·Na_4 were red-shifted by approximately 40–45 nm, as compared to the excitation spectra of NADH and NADPH reported in another study [34], which may be caused by the combination with Na. The emission spectra scanned under the maximum excitation wavelength explained that the reduced coenzymes were the dominant source of the spore autofluorescence. However, reduced coenzymes were indistinguishable because they had maximum excitation and emission wavelength in common, and an extremely similar trend and intensity. According to our results, NADP·Na_2 was not related to autofluorescence, and NAD displayed a special shape at the peak at 375 nm, which was different from the spectra of *E. quercicola* and *E. cichoracearum*. The extra peak of the spores in *P. hibiscicola* at 487 nm indicated that NAD possibly contributes to its autofluorescence. NAD(P)H has been known to be the inner probe of respiration and metabolism in cells. Conversion between NAD(P)H and NAD(P) exists in physiological cycles, and NAD(P)H is the key factor in providing energy for further processes. The accumulation of reduced coenzyme and oxidized coenzyme in their spores not only reflects the different spectral trends but also indicates the metabolic status of the conidia. Therefore, it seems that NAD(P)H monitoring better reflects the vigorousness and metabolism in organisms than other bioindicators do; however, similar life cycles cannot represent the same energy metabolism status and intrinsic contents.

The PCA analysis result demonstrated that the spectral patterns of the powdery mildew are visually distinctive and statistically separable. In related studies, PCA has been used for Raman spectroscopy and Surface-Enhanced Raman Scattering spectroscopy in fungal identification [35, 36, 37]. By contrast, we did not use complex spectral processes and cumbersome sample treatments. Furthermore, fungal autofluorescence may lead to an elevated Raman spectral baseline, masking the Raman signature. Notably, autofluorescence is a characteristic signal of fungi, recognized as an intrinsic fluorescent label [29]. The fluorescence spectra of pollen and fungal spores related to Primary Biological Aerosol Particles that were scanned and cluster-validated in PCA have been reported [38]. In this study, we not only scanned the fluorescence spectra, but also demonstrated the normalized spectral features and PCA score plots. Using the relative position and distance, we clarified that NAD may also be also a part of the source of conidial autofluorescence and that NADP is an irrelevant element. To validate this method, further research should add additional species of spores and fluorescent standards. Certainly, the new method may be restricted by the sample status and our findings that autofluorescence gradually increases with increase in number of measurements due to laser irradiation and shows a decrease in intensity value. However, this situation did not affect the trend of samples, and the reduction was mild.

In conclusion, characteristic autofluorescence provides new possibilities for in-situ and micro-samples of airborne fungal spores to avoid crop yield reduction and economic losses in agriculture. Especially for

fungi similar to powdery mildew which are obligate parasites that cannot be cultured purely, they have extremely similar morphologies, produce a large number of spores on the surface of the leaves, and spread by airborne.

5. Conclusion

Autofluorescence produced by endogenous fluorophores in organisms represents the accumulation of substances and the state of energy metabolism. In this study, we reported the visible conidial autofluorescence of three species causing powdery mildew. The fluorescence intensity represented by gray values and the emission peak at 460 nm in the spectral scan demonstrates the unique spore autofluorescence intensity features of *E. quercicola*. In addition, the autofluorescence increased sharply during the senescence of conidia in *E. quercicola* and represented accumulation of substantial fluorophores. Additionally, the conidial autofluorescence spectra of three species of powdery mildew indicate that the source is prominently contributed by NAD(P)H, and the oxidized coenzyme, NAD, is also engaged in conidial autofluorescence. These results suggest that different species of powdery mildew may be distinguished by their conidial autofluorescence. Considering that powdery mildew can produce enormous conidia on the surface of plant leaves, be spread by the wind, and infest crops causing economic losses, the autofluorescence and fluorescence spectra provide a potential application for fungi and spore identification at species level.

Declarations

Author contribution statement

Xinze Xu: Conceived and designed the experiments; Performed the experiments; Analyzed and interpreted the data; Wrote the paper.

Wenbo Liu, Weiguo Miao: Conceived and designed the experiments; Analyzed and interpreted the data; Contributed reagents, materials, analysis tools or data; Wrote the paper.

Ao Guo, Zekun Shi, Xiaobei Ji, Mengyu Fan, Xiaoli Li, Jinyao Yin: Performed the experiments; Analyzed and interpreted the data.

Zhigang Li, Xiao Li, Chunhua Lin: Contributed reagents, materials, analysis tools or data.

Funding statement

Prof.Dr. Weiguo Miao was supported by Hainan Province Science and Technology Special Fund [No. ZDYF2021XDNY142 & No. YSPTZX202018], National Natural Science Foundation of China [No. 31660033], Hainan Yazhou Bay Seed Laboratory [No. B21HJ0905].

Wenbo Liu was supported by Hainan Provincial Natural Science Foundation of China [No. 321RC470].

Xinze Xu was supported by Hainan Province Graduate Student Innovative Scientific Research Project [No. Hys2020-257].

Data availability statement

Data included in article/supp. material/referenced in article.

Declaration of interest's statement

The authors declare no conflict of interest.

Additional information

Supplementary content related to this article has been published online at https://doi.org/10.1016/j.heliyon.2022.e12084.

Acknowledgments

This study was financially supported by Hainan Province Science and Technology Special Fund (No. ZDYF2021XDNY142 YSPTZX202018); National Natural Science Foundation of China (NSFC, No. 31660033); Hainan Provincial Natural Science Foundation of China (No. 321RC470); Hainan Yazhou Bay Seed Laboratory (No. B21HJ0905); Hainan Province Graduate Student Innovative Scientific Research Project (NO. Hys2020-257).

References

[1] D. Chorvat Jr., A. Chorvatova, Multi-wavelength fluorescence lifetime spectroscopy: a new approach to the study of endogenous fluorescence in living cells and tissues, Laser Phys. Lett. 6 (2009) 410–413.

[2] S. Herbrich, M. Gehder, R. Krull, K.H. Gericke, Label-free spatial analysis of free and enzyme-bound NAD(P)H in the presence of high concentrations of melanin, J. Fluoresc. 22 (2012) 349–355.

[3] M.C. Skala, K.M. Riching, A. Gendron-Fitzpatrick, J. Eickhoff, K.W. Eliceiri, J.G. White, N. Ramanujam, In vivo multiphoton microscopy of NADH and FAD redox states, fluorescence lifetimes, and cellular morphology in precancerous epithelia, Proc. Natl. Acad. Sci. U.S.A. 104 (2007) 19494–19499.

[4] C.A. Abbas, A.A. Sibirny, Genetic control of biosynthesis and transport of riboflavin and flavin nucleotides and construction of robust biotechnological producers, Microbiol. Mol. Biol. Rev. 75 (2011) 321–360.

[5] T. Jung, A. Hohn, T. Grune, Lipofuscin: detection and quantification by microscopic techniques, Methods Mol. Biol. 594 (2010) 173–193.

[6] S.Y. Newell, Fungal biomass and productivity, Methods Microbiol. 30 (2001) 357–372.

[7] H.C. Eisenman, A. Casadevall, Synthesis and assembly of fungal melanin, Appl. Microbiol. Biotechnol. 93 (2012) 931–940.

[8] I. Strobel, J. Breitenbach, C.Q. Scheckhuber, H.D. Osiewacz, G. Sandmann, Carotenoids and carotenogenic genes in Podospora anserina: engineering of the carotenoid composition extends the life span of the mycelium, Curr. Genet. 55 (2009) 175–184.

[9] J. Wiedenmann, F. Oswald, G.U. Nienhaus, Fluorescent Proteins for Live Cell Imaging: Opportunities, Limitations, and Challenges, IUBMB Life, 2009, pp. 1029–1042.

[10] A. Baibek, M. Üçüncü, B. Short, G. Ramage, A. Lilienkampf, M. Bradley, Dyeing fungi: amphotericin B based fluorescent probes for multiplexed imaging, Chem. Commun. 57 (2021) 1899–1902.

[11] A. Muoz, M. Bertuzzi, C. Seidel, D. Thomson, N. D Read, Live-cell imaging of rapid calcium dynamics using fluorescent, genetically-encoded GCaMP probes with Aspergillus fumigatus, Fungal Genet. Biol. 151 (2020), 103470.

[12] J.A. Palero, A.N. Bader, H.S. Debruijn, d. d.H.A. Van, H.J.C.M. Sterenborg, H.C.(Gerritsen, In vivo monitoring of protein-bound and free nadh during ischemia by nonlinear spectral imaging microscopy, Biomed. Opt Express 2 (5) (2011) 1030–1039.

[13] K.R. Minker, M.L. Biedrzycki, A. Kolagunda, S. Rhein, F.J. Perina, S.S. Jacobs, M. Moore, T.M. Jamann, Q. Yang, R. Nelson, P. Balint-Kurti, C. Kambhamettu, R.J. Wisser, J.L.(Caplan, Semiautomated confocal imaging of fungal pathogenesis on plants: microscopic analysis of macroscopic specimens, Microsc. Res. Tech. (2016).

[14] P. Aguilera, F. Borie, A. Seguel, P. Cornejo, Fluorescence detection of aluminum in arbuscular mycorrhizal fungal structures and glomalin using confocal laser scanning microscopy, Soil Biol. Biochem. 43 (2011) 2427–2431.

[15] Z. Žižka, T. Vètrovský, J. Gabriel, Enhancement of autofluorescence of the brown-rot fungus piptoporus betulinus by metal ions, Folia Microbiol. 55 (2010) 625–628.

[16] V. Raimondi, L. Palombi, G. Cecchi, D. Lognoli, M. Trambusti, I. Gomoiu, Remote detection of laser-induced autofluorescence on pure cultures of fungal and bacterial strains and their analysis with multivariate techniques, Opt Commun. 273 (2007) 219–225.

[17] J. Urbanczyk, M.A.F. Casado, T.E. Díaz, P. Heras, M. Infante, A.G. Borrego, Reprint of "spectral fluorescence variation of pollen and spores from recent peat-forming plants, Int. J. Coal Geol. 139 (2015) 206–216.

[18] B. Dreyer, A. Morte, M. Pérez-Gilabert, M. Honrubia, Autofluorescence detection of arbuscular mycorrhizal fungal structures in palm roots: an underestimated experimental method, Mycol. Res. 110 (2006) 887–897.

[19] C.C. Carmarán, S. Rosenfeldt, D. Skigin, M. Inchaussandague, H.W. Keller, Autofluorescence and ultrastructure in the myxomycete diachea leucopodia (physarales), Curr. Microbiol. 67 (2013) 674–678.

[20] A.K. Neumann, M.S. Graus, J.A. Timlin, Hyperspectral fluorescence microscopy detects autofluorescent factors that can be exploited as a diagnostic method for candida species differentiation, J. Biomed. Opt. 22 (2017), 016002.

[21] R. Zhang, R. Chouket, M. Plamont, Z. Kelemen, A. Espagne, A.G. Tebo, A. Gautier, L. Gissot, J. Faure, L. Jullien, V. Croquette, T.L. Saux, Macroscale fluorescence imaging against autofluorescence under ambient light, Light Sci. Appl. 7 (2018) 2047–7538.

[22] S.H. Wen, V. Jhanji, C.Y. Dong, Confocal autofluorescence identification of bacteria, fungi, and acanthamoeba in infected porcine cornea models, Optik 168 (2018) 384–389.

[23] T. Christine, P. Gabriel, S. Corentin, Fret-slim on native autofluorescence: a fast and reliable method to study interactions between fluorescent probes and lignin in plant cell wall, Plant Methods 14 (2018) 1746–4811.

[24] L. Kiss, Natural occurrence of ampelomyces intracellular mycoparasites in mycelia of powdery mildew fungi, New Phytol. 140 (2008) 709–714.
[25] H. Wu, Y. Pan, R. Di, Q. He, M.J.N. Rajaofera, W. Liu, F. Zheng, W. Miao, Molecular Identification of the Powdery Mildew Fungus Infecting Rubber Trees in China, For. Pathol., 2019, e12519.
[26] A. Mayevsky, G.G.(Rogatsky, Mitochondrial function in vivo evaluated by NADH fluorescence: from animal models to human studies, Am. J. Physiol. Cell Physiol. 292 (2007) C615–C640.
[27] S. Limkaisang, S. Kom-un, S. Takamatsu, E.L. Furtado, K.W. Liew, B. Salleh, Y. Sato, Molecular phylogenetic and morphological analyses of Oidium heveae, a powdery mildew of rubber tree, Mycoscience 46 (2005) 220–226.
[28] T. Hirata, S. Takamatsu, Nucleotide sequence diversity of rDNA internal transcribed spacers extracted from conidia and cleistothecia of several powdery mildew fungi, Mycoscience 37 (1996) 283–288.
[29] H. Knaus, G.A. Blab, G. Jerre van Veluw, H.C. Gerritsen, H.A.B. Wösten, Label-free fluorescence microscopy in fungi, Fungal Biol Rev 27 (2013) 60–66.
[30] J.A. Palero, A.N. Bader, H.S. de Bruijn, A. van der Ploeg van den Heuvel, H.J.C.M. Sterenborg, Hans C. Gerritsen, In vivo monitoring of protein-bound and free NADH during ischemia by nonlinear spectral imaging microscopy, Biomed. Opt Express 2 (2011) 1030–1039.
[31] A.B. Canelas, W.M.v. Gulik, J.J. Heijnen, Determination of the cytosolic free NAD/NADH ratio in Saccharomyces cerevisiae under steady-state and highly dynamic conditions, Biotechnol. Bioeng. 100 (2008) 734–743.
[32] G.A. Wagnieres, W.M. Star, B.C. Wilson, In vivo fluorescence spectroscopy and imaging for oncological applications, Photochem. Photobiol. 68 (1998) 603–632.
[33] J.M. Berg, J.L. Tymoczko, L. Stryer, Biochemistry, fifth ed., W.H.Freeman & Co Ltd, 2002.
[34] P. Bondza-Kibangou, C. Millot, J. Dufer, J. Millot, Microspectrofluorometry of autofluorescence emission from human leukemic living cells under oxidative stress, Biol. Cell 93 (2001) 273–280.
[35] Veronica Egging, Jasmine Nguyen, Dmitry Kurouski, Detection and identification of fungal infections in intact wheat and sorghum grain using a hand-held Raman spectrometer, Anal. Chem. 90 (2018) 8616–8621.
[36] E. Witkowska, T. Jagielski, A. Kamińska, Genus- and species-level identification of dermatophyte fungi by surface-enhanced Raman spectroscopy, Spectrochim. Acta, Part A 192 (2017) 285–290.
[37] Q. Gan, X. Wang, Y. Wang, Z. Xie, Y. Tian, Y. Lu, Culture-free detection of crop pathogens at the single-cell level by micro-Raman spectroscopy, Adv. Sci. 4 (2017), 1700127.
[38] D.J. O'Connor, D. Iacopino, D.A. Healy, D. O'Sullivan, J.R. Sodeau, The intrinsic fluorescence spectra of selected pollen and fungal spores, Atmos. Environ. 45 (2011) 6451–6458.